JOURNAL OF MATERIALS SCIENCE 37 (2002) 699–703

Phase formation kinetics in SrO-Al_2O_3-SiO_2-B_2O_3 glass

YUN-MO SUNG
Department of Materials Science and Engineering, Daejin University, Pochun-koon, Kyunggi-do 487-711, South Korea
E-mail: ymsung@road.daejin.ac.kr

Phase formation in Sr-celsian glass, containing 3 wt% B_2O_3 (SA2SB), was investigated by using non-isothermal and isothermal kinetic analyses. While stoichiometric celsian (SA2S) glass showed two-stage crystallization of glass, from glassy state to hexacelsian and from hexacelsian to monocelsian, SA2SB glass showed direct crystallization of glass to monocelsian, resulting in considerable decrease in the temperature of monocelsian formation. The activation energy for monocelsian formation in SA2SB glass was 390 kJ/mol, which is lower than those for hexacelsian and monocelsian formation respectively in SA2S glass. The Avrami exponent of SA2SB glass was ~2.0, indicating two-dimensional crystal growth with interface-controlled mechanism at a zero nucleation rate.

1. Introduction

Strontium aluminosilicate composition forming monocelsian ($SrO \cdot Al_2O_3 \cdot 2SiO_2$: SA2S) as primary crystalline phase has been studied mainly for its use as matrix material for hightemperature ceramic composites [1, 2]. This is due to its high refractory character, low thermal coefficient of expansion (TCE) of $2.5 \times 10^{-6}/^{\circ}C$, oxidation resistance, and phase stability up to its melting temperature at 1650°C [3–8]. On the other hand, hexacelsian, which is a high-temperature metastable phase of the SA2S composition, shows a high thermal expansion coefficient of $8 \times 10^{-6}/^{\circ}C$ and reversible phase transformation in the 600°–800°C range, which is accompanied by a volume expansion of 3%. Therefore, formation of hexacelsian is undesirable in high temperature structural applications of SA2S glass-ceramics.

Bansal and Drummond [4] used x-ray diffraction (XRD) to study the kinetic of hexacelsian-to-monocelsian phase transformation in stoichiometric SA2S and reported that bulk hexacelsian, heated at 1100°C for 30 h or at 1200°C for 2 h, transformed to almost pure monocelsian. Also, they determined the activation energy for phase transformation as 527 ± 50 kJ/mol and the Avrami exponent as 0.94–1.42. Hyatt and Bansal [5] studied the crystallization kinetics of stoichiometric SA2S glass powder and determined the activation energy for hexacelsian crystal growth as 534 kJ/mol and the Avrami exponent as 4.2. By using XRD technique, they found that the phase transformation of hexacelsian to monocelsian occurs after 1 h heating at 1100°C in SA2S glass powder. Recently, Sung [6] revealed that there exist double exothermic peaks partially overlapped in DTA scan curves of stoichiometric SA2S glass. The first one, appearing at low temperature, was due to the crystallization of the parent glass to both hexacelsian and monocelsian phases and the second one, appearing at higher temperature, was due to the transformation of hexacelsian to monocelsian. However, the nature of the first peak was somewhat misinterpreted and correction is given at the present study.

The decrease in the crystallization temperature of a parent glass can give rise to huge benefit in the processing of a glass-ceramic. One of the most effective approaches for this would be to make a slight compositional change [7–11]. Knickerbocker *et al*. [10] reported that the addition of B_2O_3 or P_2O_5 into β-spodumene ($Li_2O \cdot Al_2O_3 \cdot 4SiO_2$) glass-ceramics could considerably reduce the glass viscosity above the glass transition temperature and decrease its crystallization temperature. Also, Sung [11] revealed that introduction of B_2O_3 and P_2O_5 into cordierite ($2MgO \cdot 2Al_2O_3 \cdot 5SiO_2$) glasses could prevent the formation of metastable β-cordierite, which always proceeds to α-cordierite formation in a stoichiometric cordierite glass and thus, could considerably decrease the crystallization temperatures of α-cordierite phase.

For the present study, crystallization kinetics of 97 wt% $SrO \cdot Al_2O_3 \cdot 2SiO_2$–3 wt% B_2O_3 (SA2SB) glass powder was thoroughly investigated by using isothermal and non-isothermal analyses and the result was compared with that of the stoichiometric $SrO \cdot Al_2O_3 \cdot 2SiO_2$ (SA2S) glass powder.

2. Experimental procedure

As starting materials, high purity powders of $SrCO_3$, Al_2O_3, SiO_2, and B_2O_3 were used as received from Aldrich Chemical (Milwaukee, WI). Table I shows

TABLE I Chemical composition of glass powder prepared for the present study

Glasses	Composition (wt%)			
	SrO	Al_2O_3	SiO_2	B_2O_3
SA2S	31.81	31.30	36.89	–
SA2SB	30.86	30.36	35.78	3.00

the chemical composition of the stoichiometric SA2S and SA2SB glasses investigated in the present study. The ceramic powders were mixed using zirconia-ball milling (YSZ ball mill, Nikato, Japan) for 24 h. The powder mixture was loaded into a platinum crucible and placed in a resistance furnace with super Kanthal® heating elements for glass melting. The weight of a target glass was 20 g. The powder mixture was calcined at 1000°C for 1 h, further heated to 1600°C for 1 h for complete glass melting, and quenched into distilled water. Clear glass fragments were obtained, which were dried, hand ground using a high-purity alumina mortar and pestle, and zirconia-ball milled to the average particle size of 3–5 μm.

For each glass powder, characteristic temperatures, such as glass transition (T_g) and primary (T_p) and secondary (T_p') exothermic peaks, were determined using differential thermal analyses (DTA: SETARAM TGDTA-92, France). In order to identify double exotherms in SA2S glass, glass powders were DTA rate-heated (10°C/min) up to 1016 and 1170°C respectively and rapidly cooled down (90°C/min) to room temperature. Each heat-treated glass powder was identified for phase formation using x-ray diffraction (XRD: Rigaku-2000, Japan) analysis. XRD was performed on the heat-treated glass powders with a Cu-K_α source, a 4-s time constant, a 20°–70° scan, and 0.02° step size. Phase identification was performed by comparing the 2θ values and relative peak intensities with the data listed in JCPDS cards (#38-1454 for monocelsian $SrO \cdot Al_2O_3 \cdot 2SiO_2$ and #35-73 for hexacelsian $SrO \cdot Al_2O_3 \cdot 2SiO_2$).

DTA scans at the heating rates of 5, 10, 15, 20 and 30°C/min, were performed on the glass powders up to 1500°C. The DTA results were analyzed to calculate the activation energy for phase transformation and nucleation/crystallization mode, using non-isothermal kinetic equations. Also, glass powders were isothermally heated at 955, 960, 965, 970, and 975°C, respectively using DTA and isothermal kinetics analyses were applied to determine the kinetic parameters. XRD was also performed on the heat-treated glass powders with the same conditions.

3. Results

3.1. Non-isothermal kinetics

Typical DTA curves of the SA2S and SA2SB glass powders at a heating rate of 20°C/min are shown in Fig. 1a and b, respectively. The second peak, appearing in the DTA scan curves of the SA2S glass powder, disappeared in the SA2SB glass scan. Table II shows the glass transition (T_g) and crystallization peak temperatures (T_p, T_p') at different heating rates for SA2S and SA2SB glasses as determined by DTA. The primary and secondary peaks in the DTA scan curves of SA2S glass powder were identified by XRD on the glass powders heated up to 1016° and 1170°C, respectively. The temperature of 1016°C is between the crystallization onset (T_o) and the primary peak temperature (T_p) and at this temperature, the primary and the secondary peaks are not overlapped. The temperature of 1170°C is higher than the completion temperature of the secondary peak. Thus, the glass powder, heated up to 1016°C, must present the nature of the primary crystallization peak and the glass powder heated up to 1170°C, must present the nature of the secondary peak. Fig. 2 shows XRD patterns of SA2S glass powder heated up to 1016° (a) and 1170°C (b), respectively, and SA2SB glass powder heated up to 1008°C (c). The SA2S glass powder, heated up to 1016°C, shows the presence of hexacelsian as only crystalline phase and that, heated up to 1170°C, shows the presence of monocelsian with a small amount of glassy phase. On the other hand, XRD pattern of the SA2SB glass powder, heated up to T_p, shows only monocelsian phase.

TABLE II Glass transition (T_g) and crystallization peak temperatures (T_p, T_p') of glass powder prepared for the present study

Scan rate (°C/min)	Glasses					
	SA2S			SA2SB		
	T_g	T_p	T_p'	T_g	T_p	T_p'
5	860	1022	1095	815	988	–
10	877	1037	1115	818	1008	–
15	880	1045	1123	833	1025	–
20	881	1052	1132	836	1031	–
30	880	1062	1144	838	1044	–

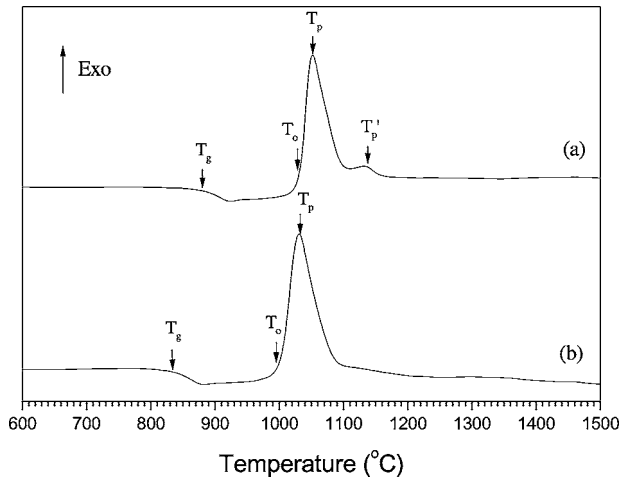

Figure 1 Differential thermal analysis (DTA) scan curves of (a) SA2S and (b) SA2SB glass powders at a scan rate of 20°C/min.

The DTA peak temperatures (T_p, T_p'), the heating rate (ϕ), and activation energy for phase transformation (Q) can be related, following Kissinger [12], as,

$$\ln\left(\frac{\phi}{T_p^2}\right) = -\frac{Q}{RT_p} + \text{const.} \quad (1)$$

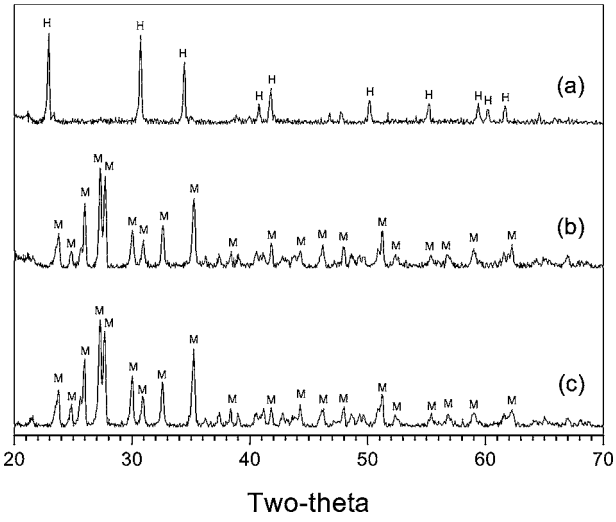

Figure 2 X-ray diffraction (XRD) patterns of SA2S glass powder heated up to 1016° (a) and 1170°C (b) and SA2SB glass powder heated up to 1008°C (c). Here, H and M denote hexacelsian and monocelsian phases, respectively.

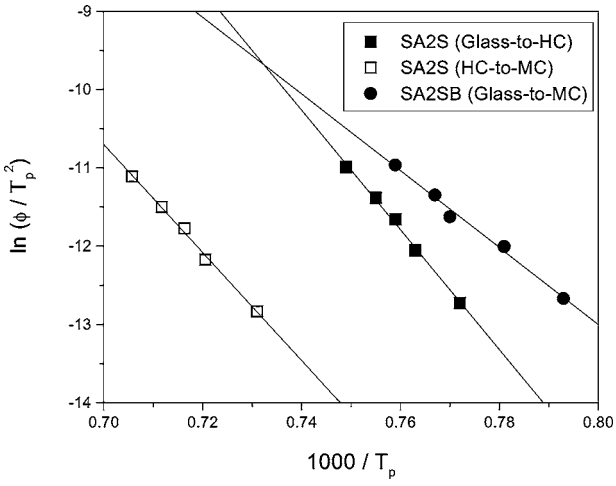

Figure 3 Kissinger plots for the transformations: glass to hexacelsian (HC) and hexacelsian (HC) to monocelsian (MC) in SA2S, and glass to monocelsian (MC) in SA2SB glass powder.

where R is the gas constant. Fig. 3 shows Kissinger plots of ln (ϕ/T_p^2) vs. $1000/T_p$ for the SA2S and SA2SB glasses. For the SA2S glass, plots for the crystallization of hexacelsian (T_p) and phase transformation of hexacelsian to monocelsian (T_p') were plotted together. Activation energy for the crystallization of hexacelsian in SA2S glass powder was determined as 636 kJ/mol from the slope $(-Q/R)$ of the plot. Activation energy for the phase transformation from hexacelsian to monocelsian was determined as 573 kJ/mol. Also, for the SA2SB glass powder, activation energy for the crystallization of monocelsian was determined as 408 kJ/mol.

The order of reaction or transformation, n, also known as Avrami exponent, was determined for the SA2S and SA2SB glasses using a method given by Ozawa [13]

$$\ln[-\ln(1-x)]_T = -n\ln\phi + \text{const.} \qquad (2)$$

where x is the volume fraction crystallized at a fixed temperature, T, and ϕ is the DTA scan rate. Here, T was

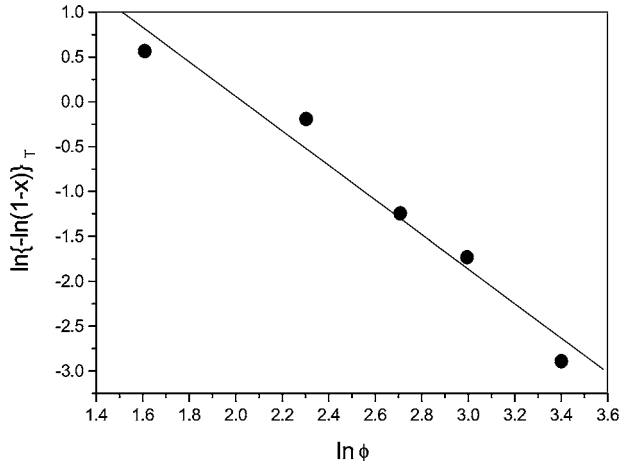

Figure 4 An Ozawa plot for the glass-to-monocelsian transformation in SA2SB glass powder.

1020°C. Fig. 4 shows the Ozawa plots of the SA2SB glass powder. From slope of the curve, Avrami exponent (n) was determined as 1.92. For DTA curves of SA2S glass powder, two exothermic peaks were overlapped, hence this Ozawa analysis was not applicable. A method given by Augis-Bennett [14] was used to calculate n for the transformation of SA2S glass.

$$n = \frac{2.5\,RT_p^2}{\delta\,Q} \qquad (3)$$

where δ is width of the DTA peak at half the peak height. The values of n determined using Equation 3 were 1.87 and 2.01 for the SA2S and SA2SB respectively.

3.2. Isothermal kinetics

The isothermal kinetics of Johnson-Mehl-Avrami (JMA) analysis was applied to the SA2SB glass powder isothermally heated at 955, 960, 965, 970, and 975°C until crystallization completes. Fig. 5 shows a typical DTA isothermal heating (970°C) curve of SA2SB glass powder. The fractions, reacted at different temperatures

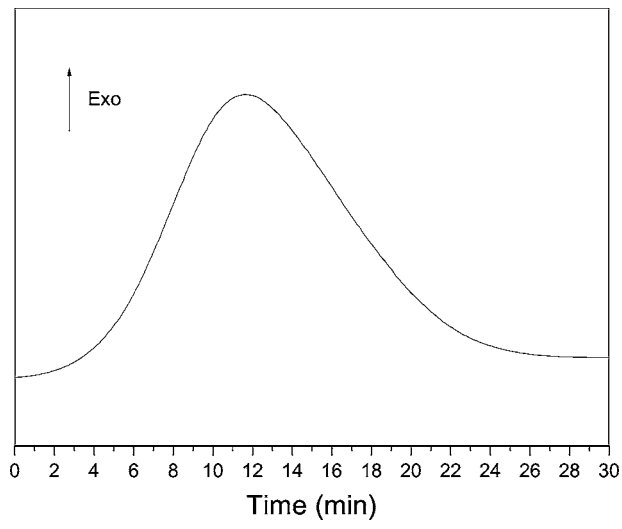

Figure 5 A typical DTA isothermal heating curve of SA2SB glass powder at 700°C.

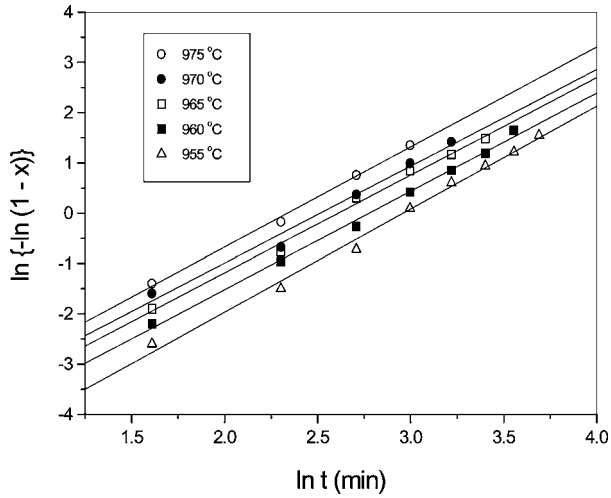

Figure 6 Johnson-Mehl-Avrami (JMA) plots for the glass-to-monocelsian transformation in SA2SB glass powder, isothermally heated at 955, 960, 965, 970 and 975°C, respectively.

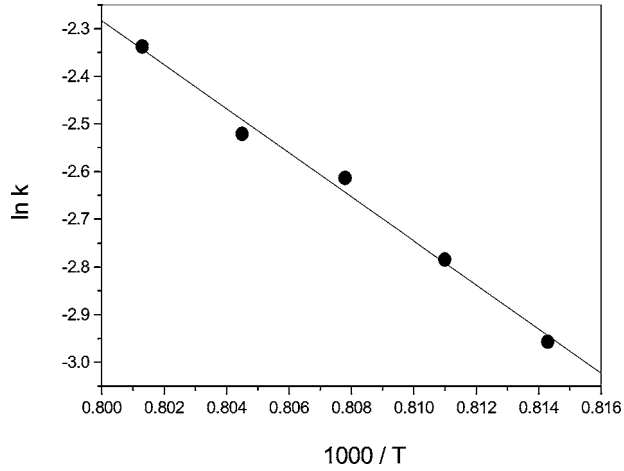

Figure 7 An arrhenius plot of SA2SB glass powder, showing activation energy for phase formation.

for each isothermal heating curve, were used for following JMA analysis [14]

$$x = 1 - \exp[-(kt)^n] \quad (4)$$

where x is the fraction reacted, k is the reaction rate constant, t is the time passed, and n is the Avrami exponent. By taking natural logarithm for both sides of Equation 4, JMA equation can be rewritten as

$$\ln[-\ln(1-x)] = n \ln k + n \ln t \quad (5)$$

By plotting $\ln[-\ln(1-x)]$ vs. $\ln t$, the Avrami exponents (n) can be obtained from the slopes of the curves. Fig. 6 shows the JMA plot for SA2SB glass powder. The values of n, determined from the slope of the straight lines in Fig. 6, ranged from 1.92 to 2.05. Here, $\ln k$ values can be obtained from the Y-intercept of the curves of the JMA plots and defined as following Arrhenius equation

$$\ln k = \ln k_o - \left(\frac{Q}{RT}\right) \quad (6)$$

where k_o is the pre-exponential constant, Q is the activation energy, and T is the absolute temperature. By plotting Arrhenius plots, as shown in Fig. 7, the activation energy for crystallization of SA2SB glass powder was determined as 384 kJ/mol. Table III lists activation energy and Avrami exponent values for SA2S and SA2SB glass powders, respectively.

4. Discussion

SA2S glass powder showed crystallization of hexacelsian phase at a low temperature followed by transformation to monocelsian. On the other hand, SA2SB glass powder showed crystallization of monocelsian directly from its parent glass at lower temperature than SA2S glass. Since the oxygen coordination around each B^{3+} ion in an oxide glass is only three, the basic structural unit, formed between B^{3+} and O^{2-} ions, is almost two-dimensional BO_3 triangle. Thus, introduction of B_2O_3 into the alkali aluminosilicate glass would reduce the degree of three-dimensional connectivity that is, viscosity [16]. The lowered T_g values in SA2SB glass powder are the evidence of the reduced connectivity in the glass. The reduced connectivity between ions could decrease the activation energy for crystallization and thus, decrease the crystallization temperature as well. The reduced connectivity must have depressed formation of intermediate hexacelsian phase, which always occurs prior to the formation of monocelsian phase in the case of SA2S glass. Thus, the T_p' and T_p correspond to the temperatures for monocelsian formation in SA2S and SA2SB glass powders, respectively and the difference between them is approximately 100°C. The effect of B_2O_3 addition is apparent in the decreasing crystallization temperature. The activation energy for crystallization of hexacelsian phase in SA2S glass powder was 636 kJ/mol, which is relatively higher than the value of 534 kJ/mol from the result of Bansal *et al.* [5]. The activation energy for transformation of hexacelsian to monocelsian in SA2S glass

TABLE III Avrami exponent (n) and activation energy (Q) for phase formation in the glass powders prepared for the present study

	Avrami exponent			Activation energy (kJ/mol)		
Glasses	G-H[a]	H-M[b]	G-M[c]	G-H[a]	H-M[b]	G-M[c]
SA2S	1.87(4.2)[d]	(1.1)[e]	–	636 (534)[d]	573 (527)[e]	–
SA2SB	–	–	1.92–2.05	–	–	384–408

[a]Glass to Hexacelsian.
[b]Hexacelsian to Monocelsian.
[c]Glass to Monocelsian.
[d]Data from Hyatt and Bansal [5].
[e]Data from Bansal and Drummond, III [4].

powder, determined by using Kissinger analysis, was 573 kJ/mol, which is in accordance with Bansal *et al.*'s result of 527 kJ/mol, obtained using JMA analysis. The transformation of hexacelsian to monocelsian requires the structural change from two dimensional sheet structure of hexacelsian to three dimensional network structure of monocelsian. This procedure must involve the breaking of Si-O and Al-O bonds. Here, the dissociation energy for Si-O bonds is 445 kJ/mol and that for Al-O bonds is 330–423 kJ/mol [17]. Thus, the activation energy for transformation, 573 kJ/mol is higher than the dissociation energy values for the ion bonds. For the phase transformation, diffusion of ions is involved and for the diffusion of ions to occur, two procedures must be involved, dissociation of ions and migration of dissociated ions. Thus, the activation energy is summation of the energy values required for each procedure. The activation energy margin of 128 kJ/mol could correspond to the energy for the ion migration. For SA2SB glass powder, the activation energy for formation of monocelsian directly from its parent glass was determined as 408 kJ/mol and 384 kJ/mol by Kissinger and JMA analyses, respectively. These values are lower than the crystallization energy for hexacelsian phase and the transformation energy from hexacelsian to monocelsian phase. Again, the decreased connectivity between ions, caused by addition of B_2O_3, would have reduced the activation energy for crystallization of SA2SB glass powder.

The crystallization mode of a glass can be estimated by analyzing Avrami exponent (n) and it can be expressed as following [18]

$$n = a + mb \tag{7}$$

where a refers to the nucleation rate with the value 1 for constant nucleation rate, 0 for zero nucleation rate, $a > 1$ for an increasing nucleation rate and $a < 1$ for a decreasing nucleation rate, m corresponds to the dimensionality of the crystal growth, and b relates to the mechanism of growth with the value 1.0 for an interface-controlled process and 0.5 for a diffusion-controlled process. For the present study, Avrami exponent (n) of SA2SB glass powder was determined as 1.92–2.05, using Ozawa, JMA and Augis-Bennett analyses. The value of ~ 2 implies that the crystallization of monocelsian phase occurs at a zero nucleation rate ($a = 0$). The dimension of crystals is two ($m = 2$), indicating plate-like grains, and the crystallization is an interface-controlled process ($b = 1$). Since there is no apparent compositional change across the interface between parent glass and monocelsian crystals during crystallization procedure, the crystal growth by the interface-controlled mechanism would highly be the case rather than diffusion-controlled mechanism. The nucleation and crystal growth mode of glass-to-monocelsian crystallization in SA2SB glass powder was similar to that of glass-to-hexacelsian crystallization in SA2S glass powder. For the present study, by using Augis-Bennett analysis, Avrami exponent of glass-to-hexacelsian transformnation in SA2S glass was determined as 1.87, which also implies the two-dimensional hexacelsian crystal growth at a zero nucleation rate with interface-controlled mechanism. However, this result is contradictory to that of Hyatt and Bansal [5] and they obtained Avrami exponent of 4.2 by using Piloyan *et al.*'s analysis [19].

5. Summary

SA2SB glass powder showed direct crystallization to monocelsian, while stoichiometric SA2S glass powder showed two-step phase transformation of glass, from glassy state to hexacelsian and from hexacelsian to monocelsian. As this result, the monocelsian formation temperature in SA2SB glass powder was decreased in $\sim 100^{\circ}$C compared to that of SA2S glass powder. The activation energy for monocelsian phase formation in SA2SB powder was determined as 384–408 kJ/mol, which is lower than that for crystallization of glass to hexacelsian phase (636 kJ/mol) and that for phase transformation of hexacelsian to monocelsian (573 kJ/mol), respectively in SA2S glass powder. This implies that the number of Si-O and Al-O broken bonds was increased by addition of B_2O_3 into SA2S glass powder. Avrami exponent of SA2SB glass powder was determined as ~ 2.0, indicating two-dimensional crystal growth with interface-controlled mechanism at a zero nucleation rate.

Acknowledgements

The author would like to thank Mr. Jong-Sub Lee and Mr. Kee-Chun Shin at Daejin University for their assistance in performing experiments. The author also thanks a reviewer for his or her English correction.

References

1. N. P. BANSAL, *J. Mater. Res.* **12** (1997) 745.
2. *Idem., Mater. Sci. & Eng.* **A231** (1997) 117.
3. N. P. BANSAL, M. J. HYATT and C. H. DRUMMOND, III, *Ceram. Eng. Sci. Proc.* **12** (1991) 1222.
4. N. P. BANSAL and C. H. DRUMMOND, III, *J. Amer. Ceram. Soc.* **76** (1993) 1231.
5. M. J. HYATT and N. P. BANSAL, *J. Mater. Sci.* **31** (1996) 172.
6. Y.-M. SUNG, *J. Mater. Sci. Lett.* **19** (2000) 453.
7. Y.-M. SUNG and S. KIM, *ibid.* **35** (2000) 4293.
8. Y.-M. SUNG and J. S. PARK, *ibid.* **34** (1999) 5803.
9. Y.-M. SUNG and J.-W. AHN, *J. Mater. Sci.* **35** (2000) 4913.
10. S. KNICKERBOCKER, M. R. TUZZOLO and S. LAWHORNE, *J. Amer. Ceram. Soc.* **72** (1989) 1873.
11. Y.-M. SUNG, *J. Mater. Sci.* **31** (1996) 5421.
12. H. E. KISSINGER, *J. Res. Natl. Bur. Stand.* (U.S.) **57** (1956) 217.
13. T. OZAWA, *Polymer* **12** (1971) 150.
14. J. A. AUGIS and J. E. BENNETT, *J. Thermal Anal.* **13** (1978) 283.
15. M. AVRAMI, *J. Chem. Phys.* **7** (1939) 1103.
16. Y.-M. SUNG, S. A. DUNN and J. A. KOUTSKY, *J. Eur. Ceram. Soc.* **14** (1994) 455.
17. W. D. KINGERY, H. K. BOWEN and D. R. UHLMANN, "Introduction to Ceramics," 2nd edn. (Wiley, New York, 1976) p. 99.
18. Y.-M. SUNG, *J. Mater. Res.* **16** (2001) 2039.
19. G. O. PILOYAN, I. D. RYBACHIKOV and O. S. NOVIKOVA, *Nature* **212** (1996) 1229.

Received 12 April
and accepted 2 October 2001